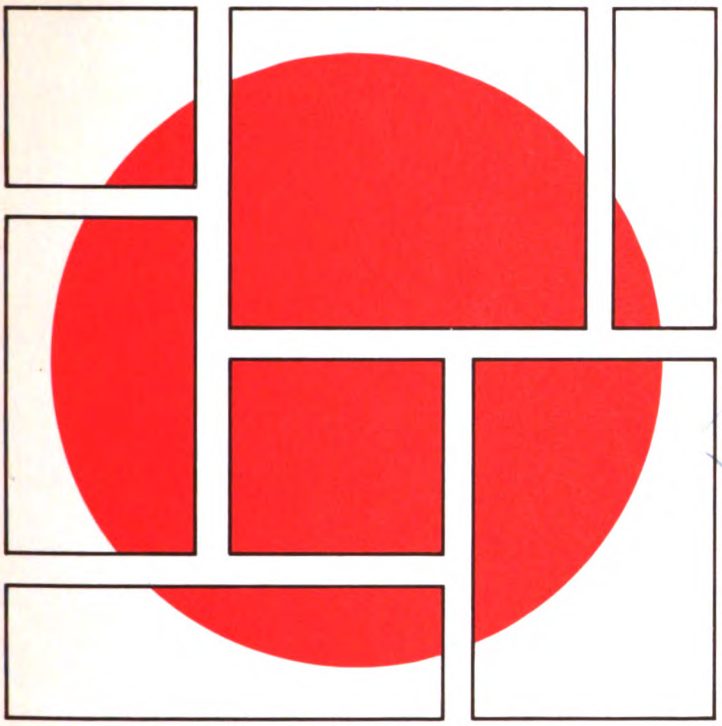

Short Papers on Research in 1977

Bulletin 211 Part 4

Kansas Geological Survey
The University of Kansas
Lawrence, Kansas 66044

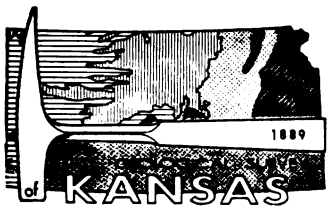

BULLETIN 211, PART 4

Short Papers on Research in 1977

Compiled by
Gary A. Waldron

Printed by authority of the State of Kansas
Distributed from Lawrence

UNIVERSITY OF KANSAS PUBLICATIONS
APRIL 1978

Short Papers on Research in 1977

This collection of papers renews a series published by the Survey from 1967-1971 as a part of the Reports of Studies in the Bulletin. The papers present technical and scientific results of work by members of the Kansas Geological Survey during 1976 and 1977.

Contents

GERARD W. JAMES

Uranium and Thorium in Volcanic Ash Deposits of Kansas:
Implications for Uranium Exploration in the Central Great Plains

ABSTRACT

Fourteen samples of unaltered Pliocene and Pleistocene volcanic ashes contain an average of 7.1 ppm uranium and 33.2 ppm thorium; four devitrified ashes contain an average of 5.2 ppm uranium and 21.6 ppm thorium.

Dissolution and/or leaching of uranium from the abundant ash beds may account for the high regional background values of uranium (5-20 ppb) found in groundwaters of western Kansas. The rhyolitic ashes are also the likely source of silica found in the widespread uraniferous (10-200 ppm) silcrete deposits in the lower Ogallala Formation.

Fluvial sandstones with organic reductants that could have been in hydrologic contact with uraniferous waters include the Lower Cretaceous Cheyenne, Kiowa, and Dakota Formations of north-central and southwestern Kansas.

INTRODUCTION

The close association of tuffaceous rock units with many sedimentary uranium deposits has led several investigators [e.g. 1,2] to postulate leaching of these types of rocks as a likely source of uranium which can be mobilized by meteoric or groundwaters, and subsequently fixed by interaction with organic reductants. Although there is only limited data available in the literature to support the leaching concepts [3,4], experimental work in progress [5] indicates substantial percentages of volcanic glass may go totally into solution, or that selective leaching of uranium may take place, depending on the degree of silica saturation of the leach solutions.

Lenticular deposits of volcanic ash in the Miocene, Pliocene, and Pleistocene in the fluvial and alluvial sediments of the central Great Plains have been described as relatively unaltered vitric tuffs with rhyolitic chemical compositions; attain maximum thicknesses of 30 feet; and constitute an estimated 3% of the volume of the sediments in portions of the Ogallala Formation [6,7,8]. Dissolution and/or leaching of the Great Plains ashes could have easily mobilized several millions of pounds of uranium which might be available for the formation of uranium deposits, given suitable mechanisms of fixation. That this has taken place is indirectly supported by (1) the anomalously high regional background values of uranium (5-20 ppb) found in groundwaters of western Kansas [9,10], (2) the widespread occurrences of uraniferous (10-200 ppm) silcrete deposits found in close proximity to the abundant ash beds in the lower portion of the Ogallala Formation [11,12,13], and (3) the occurrences of anomalous concentrations (10-15 ppm U) found in limonitic and hematitic sandstones of the Lower Cretaceous [11].

The purpose of this report is to present the results of preliminary investigations of the distribution of uranium and thorium in volcanic ashes in Kansas and to discuss the possible implications for uranium exploration in the central Great Plains.

Uranium and Thorium in Volcanic Ashes

The uranium and thorium contents of eighteen Pliocene and Pleistocene volcanic ashes were determined by x-ray spectrometry [14,15]; the results of these analyses are presented in Table I. The uranium values range from 3.9 to 9.1 ppm U and average 6.6 ppm; the thorium values range from 17.8 to 39.6 ppm Th and average 30.6 ppm. The Th/U ratios range from 3.8 to 5.3 and average 4.6. The estimated standard errors at the 95% confidence level for these determinations are 1.2 ppm U and 1.6 ppm Th.

Most of the ash samples analyzed can be classified as virtually unaltered glasses, and have the petrographic and optical properties typical of most ashes previously described and illustrated [e.g. 8]. X-ray

Table I. Uranium and Thorium Contents of Volcanic Ashes.

Sample	*Ash Bed*	*U ppm*	*Th ppm*	*Th/U*	*D.I.*°
Pleistocene—Pearlette Ash					
1		7.2	34.2	4.8	0.2
2		6.0	31.8	5.3	0.2
3		6.9	33.3	4.8	0.2
4		7.8	35.0	4.5	0.1
5		3.9	17.8	4.6	3.6
6		6.3	28.6	4.5	0.5
7		7.3	33.8	4.6	0.3
8		5.5	23.3	4.2	1.6
Pliocene—Ogallala Fm.—Ash Hollow Mbr.					
9	Reamsville	7.3	36.7	5.0	0.2
10	Reamsville	7.2	31.9	4.4	0.7
11	Reager	6.8	30.9	4.5	0.1
12	Reager	5.7	29.6	5.2	0.3
13	Dellvale	4.7	20.5	4.4	2.2
14	Rawlins	6.7	30.7	4.6	0.1
15	Rawlins	7.0	34.9	5.0	0.1
Pliocene—Ogallala Fm.—Valentine Mbr.					
16	Calvert	9.1	39.6	4.4	0.1
17	Calvert	6.6	24.8	3.8	2.8
18	Un-named	7.4	33.3	4.5	0.8

° Devitrification Index

diffraction examinations of these samples reveal a few in moderate to advanced stages of devitrification (samples 5, 8, 13, & 17), although none have been mineralogically altered to expanding clays. A semi-quantative devitrification index, based on the ratio of the crystalline diffraction responses of quartz and feldspars to the amorphous silica glass background, is also presented in Table I. The four devitrified ashes contain an average of 5.2 ppm uranium and 21.6 ppm thorium; the fourteen fresh ashes contain an average of 7.1 ppm U and 33.2 ppm Th.

Discussion of Results

The devitrified ash samples appear to have significantly lower uranium and thorium contents; whether this is due to devitrification effects or differences in source composition cannot be resolved with the present data. Because of presumed redeposition by fluvial systems, the detailed stratigraphic correlations of most Great Plains ashes are tenuous, unless they have been correlated by absolute geochronological dating. Fission-track dating [16] indicates the Pearlette ash beds actually consist of four significantly different ages of ash, and preliminary age data on the late Tertiary ashes suggest alternative interpretations of the stratigraphic assignments. Although some of the ash samples are thought to be the same ash beds, interpretation based on the possible loss of uranium and thorium with devitrification cannot be conclusive until absolute age dating techniques are utilized to define co-existing ash sample suites.

It should be noted, however, that studies of uranium in suites of co-existing obsidian-perlite-felsite [4] indicate no loss of uranium in the hydration of obsidian to perlite, but with devitrification show uranium depletions up to 80% in felsites, relative to the co-existing obsidians and perlites.

Implications for Uranium Exploration

The high levels of uranium found in the groundwater and the occurrences of uraniferous silcretes gives indirect support for the mobilization of uranium by dissolution and/or leaching of the volcanic ashes. Considering the prevalent concepts of the formation of uranium ore bodies in sandstones leads one to think in terms of potential host-rocks with suitable organic reductants. The Ogallala Formation does not appear to contain the required association of organic debris [17]. The pyritic and organic-debris containing fluvial sands of the Lower Cretaceous of the Great Plains that are now, or have been, in hydrologic contact with Pliocene, Pleistocene, and/or Recent uraniferous groundwaters, either through fractures or erosional contacts, should be considered potential host facies for uranium ore bodies. The depositional environments and the petrographic characteristics of the deltaic and fluvial systems of the Cheyenne, Kiowa, and Dakota Formations of Kansas are reasonably well-known [e.g. 18,19,20], and the variety of types of cementation in the sandstones (limonitic, hematitic, siliceous, and calcareous) indicates different interactions between the rocks and secondary solutions have taken place.

Conclusions

The Late Tertiary and Pleistocene volcanic ashes of the central Great Plains should be considered a uranium source facies from which uraniferous Pliocene, Pleistocene, and Recent waters have been derived. Potential uranium-bearing fluvial sandstones with organic reductants that could have been in hydrologic contact with these groundwaters include the Lower Cretaceous sands of north-central and southwestern Kansas.

LITERATURE CITED

1. H. H. Adler, "Formation of Uranium Ore Deposits," Int'l. Atomic Energy Agency, Vienna, 1974, pp. 141-168.

2. A. R. Dahl and J. L. Hagmaier, "Formation of Uranium Ore Deposits," Int'l. Atomic Energy Agency, Vienna, 1974, pp. 201-218.

3. K. A. Dickinson, U.S. Geol. Surv. Open File Report 75-595 (1975).

4. R. A. Zielinski, U.S. Geol. Surv. Open File Report 75-595 (1975).

5. R. A. Zielinski, personal communication.

6. A Swineford and J. C. Frye, Kan. Geol. Surv. Bull. 64, pt. 1 (1946).

7. J. S. Carey *et al.*, Kan. Geol. Surv. Bull. 96, pt. 1 (1952).

8. A. Swineford *et al.*, Jour. Sed. Petr., 25, 4, 243 (1955).

9. L. R. Hathaway and G. W. James, Anal. Chem., 47, 12, 2035 (1975).

10. L. R. Hathaway and G. W. James, unpublished data.

11. G. W. James, unpublished data.

12. P. Berendsen, unpublished data.

13. J. C. Frye and A. Swineford, Kan. Geol. Surv. Bull. 64, pt. 2 (1946).

14. G. W. James and L. R. Hathaway, "Exploration for Uranium Ore Deposits," Int'l. Atomic Energy Agency, Vienna, 1976, pp. 311-320.

15. G. W. James, Anal. Chem. 49, 967-969 (1977).

16. J. Boellstorff, Kan. Geol. Surv. Guidebook Ser. 1, 37 (1976).

17. J. C. Frye *et al.*, Kan. Geol. Surv. Bull. 118 (1956).

18. A Swineford, Kan. Geol. Surv. Bull. 70, pt. 4 (1947).

19. P. C. Franks, "Cretaceous Systems in the Western Interior of North America," Geol. Assoc. Canada, Sp. Paper 13, 1975, pp. 469-521.

20. C. T. Siemers, Jour. Sed. Petr., 46, 1, 97 (1976).

APPENDIX

Sample Number	Sample Locations Township-Range	County
1	21-13S-26W	Gove
2	21-13S-26W	Gove
3	1-30S-36W	Grant
4	1-30S-36W	Grant
5	1-30S-36W	Grant
6	24-30S-35W	Haskell
7	6-31S-26W	Meade
8	14- 3S-35W	Rawlins
9	32- 1S-14W	Smith
10	2- 3S-33W	Rawlins
11	2- 3S-25W	Norton
12	2- 3S-33W	Rawlins
13	35- 3S-24W	Norton
14	4- 4S-34W	Rawlins
15	30- 1S-19W	Philips
16	25- 2S-22W	Norton
17	33- 3S-34W	Rawlins
18	25- 2S-25W	Norton

H. L. STRIMPLE[1]
PHILIP H. HECKEL[1, 2]

A Significant Acrocrinid (Crinoidea: Camerata) from the Ladore Shale (Missourian, Upper Pennslyvanian) in Eastern Kansas

ABSTRACT

A rare camerate crinoid, *Planacrocrinus klapperi* n. sp., has been found in close association with a clump of linoproductid brachiopods in the Ladore Shale in Linn County, Kansas. This is the first recording of the complete crown of any species of *Planacrocrinus*. The arms are remarkably similar to those of more common inadunate crinoids.

INTRODUCTION

Only a remnant of the vast hordes of camerate crinoids that existed in Early and Middle Mississippian time survived into the Pennsylvanian. Of these the Acrocrinidae are the most common. Nevertheless, compared to the inadunate and flexible crinoids in Pennsylvanian rocks, acrocrinids are quite rare and small in size. In any event, acrocrinids are an enigma in that they are the only group among all crinoids in which the cup increases in length throughout life by the intercalation of plates between radials and basals. Newly formed intercalaries appear along the distal rim of the basal circlet and are both radial and interradial in position. It appears that acrocrinids evolved from dichocrinids through *Protacrocrinus* Moore & Strimple, 1969, of Kinderhookian (Early Mississippian) age.

Of all the unusual modifications adopted by the acrocrinids, perhaps the most unexpected is development of a radial articular facet resembling those of such inadunate crinoids as *Erisocrinus* and *Delocrinus*, wherein the facet occupies full width of the plate, extending well inward from the outer margin and possessing ligament fossae, transverse ridge, muscle attachment areas and intermuscular notch. These features have been reported for *Planacrocrinus* Moore & Strimple (1969, p. 15, fig. 6, 8) and *Platyacrocrinus* Moore & Strimple (1969, p. 10, fig. 4) from the Lower Pennsylvanian (Morrowan). These are the only genera of the entire class Camerata to have developed this type of radial articular facet. A detached set of arms was designated as a paratype of *Planacrocrinus knappi* Strimple (1975, fig. 17, *1*) from the Burgner Formation (Atokan) of Missouri; however, assignment to the species was made on the basis of crowns of the new undescribed specimens from the Ladore Shale of Kansas, which are herein described as *P. klapperi*. This new discovery extends the range of *Planacrocrinus* into the lower part of the Missourian Stage, the lower stage of the Upper Pennsylvanian Series.

The Ladore Shale in central Linn County, Kansas, is 4 to 5 feet (1.2-1.5 m) of sandy calcareous gray shale that carries thin layers of argillaceous calcilutite in the upper part (Fig. 1). The only common and conspicuous fossils in the Ladore in this region occur in the lower part at the acrocrinid locality and constitute an assemblage of brachiopods, rhomboporid bryozoans and bivalves strongly dominated by the brachiopod *Derbyia*. Other identified brachiopods in this assemblage include *Neospirifer* and a dictyoclostid. The acrocrinids were found in a clump of linoproductid brachiopods (Fig. 2) that was collected above the derbyiid assemblage in the lower of two thin calcilutite layers in the Upper Ladore. The only other fossil material in either limestone layer consists of rare and scattered tiny gastropods, echinoderm ossicles, ostracodes and a probable bivalve fragment, all noted in thin section. Slight color mottling suggests some burrowing of the substrate.

Within the Kansas cyclic sequence, the Ladore is an "outside shale member" deposited during a period of general marine regression between the widespread inundations that gave rise to the Hertha and Swope Limestones (Heckel and Baesemann, 1975, p. 493). Although "outside shales" locally contain nonmarine deposits, many of them in eastern Kansas were de-

[1] The University of Iowa, Iowa City, Iowa 52242.
[2] Also part-time with Kansas Geological Survey, Lawrence, Kansas 66044.

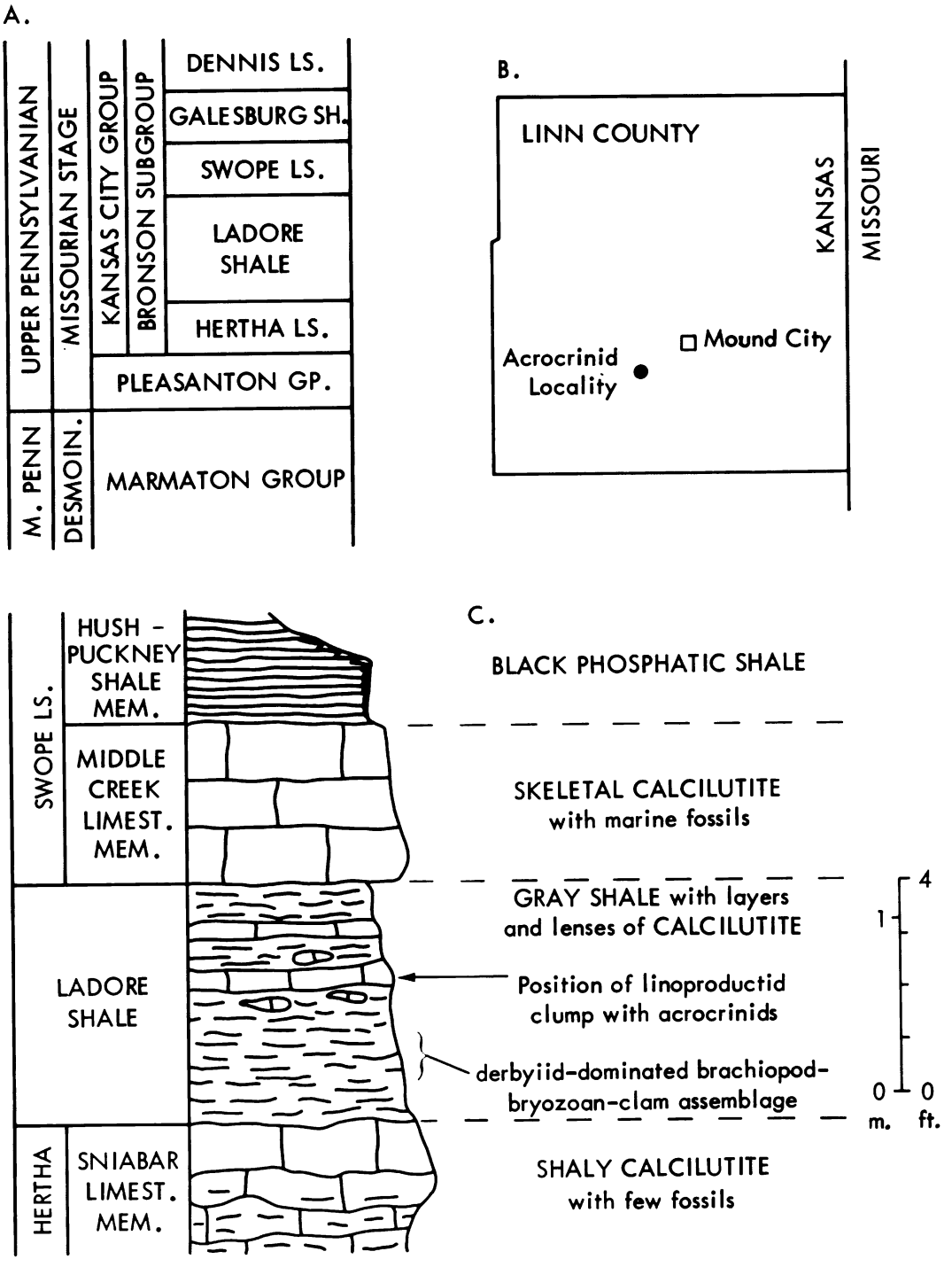

FIGURE 1.—Location of acrocrinid collection. A. Position of Ladore Shale in Upper Pennsylvanian sequence of eastern Kansas. B. Linn Co., Kansas, showing acrocrinid locality about 2 miles (3 km) southwest of Mound City. C. Measured section of Ladore Shale at acrocrinid locality on north side of Kansas Hwy. 52, in NE¼ SW¼ sec. 23, T22S, R23E.

posited in nearshore portions of a sea that was merely reduced in size and subject to greater detrital influx than during more inundative phases. Thus, these acrocrinids lived in a marine environment that received enough mud influx that the turbid water and soft substrate was unfavorable to most sessile organisms. This, along with detrital dilution, accounts for the general scarcity of fossils in most of the Ladore. Only when the clump of several linoproductid brachiopods became established on the sea bottom was a local area of substrate favorable for growth of the acrocrinids.

P. klapperi is represented by three small crinoids which have articulated stalks (columns) and arms. One specimen (Fig. 3, 4), the holotype (SUI 35580), which has been removed from the shaly matrix of the clump, is a perfect crown with the proximal portion of the column attached. There is little doubt that the crinoids were living in association with the linoproductid brachiopods, which probably had formed a tiny mound above the muddy substrate. Because crinoids are filter feeders, they require relatively good water circulation. Very likely these acrocrinids benefited from the mini-currents set up by the several linoproductids as well as from the more stable substrate that the large brachiopods offered. The only other instance of intimate association between large brachiopods and crinoids known to us is in an exposure of the Barnett Hill Member, Atoka Formation, Atokan Stage (Middle Pennsylvanian) in Coal County, Oklahoma, in which the matrix is weakly calcareous sandstone, heavily impregnated with iron oxide. Specimens of *Oklahomacrinus, Stellarocrinus, Elibatocrinus, Isollagecrinus* and other genera have been found embedded with, and even inside, disarticulated valves of productids. It seems that both the Kansas and Oklahoma occurrences were buried by a rapid influx of mud that entombed the crinoids instantly and protected them from the ravages of scavengers. Complete disarticulation of the myriad of plates forming the endoskeletons of crinoids is known to take place in a matter of several days if they are left exposed on the sea floor after death (Meyer, 1971).

SYSTEMATIC PALEONTOLOGY

Class CRINOIDEA Miller, 1821
Subclass CAMERATA Wachsmuth & Springer, 1885
Order MONOBATHRIDA Moore & Laudon, 1943
Superfamily HEXACRINITACEA Wachsmuth & Springer, 1885
Family ACROCRINIDAE Wachsmuth & Springer, 1885
Subfamily ACROCRININAE Wachsmuth & Springer, 1885
Genus PLANACROCRINUS Moore & Strimple, 1969

Type species. Planacrocrinus ambix Moore & Strimple, 1969, p. 15.

Diagnosis (after Moore & Strimple, 1969). Calyx

FIGURE 2.—Cluster of linoproductid brachiopods with stems and crowns of *Planacrocrinus* klapperi n. sp. (SUI 43157) on upper surface. Holotype of *P. klapperi* has been removed and is illustrated elsewhere.

flat at base and summit, bowl-shaped to subconical with steep nearly straight sides, basals clearly visible in side view; radials wider than high, with straight articular facets occupying full width of plates and extending well inward from outer margin, resembling facets of such inadunate crinoids as *Delocrinus* and *Cromyocrinus* in presence of ligament fossae, transverse ridge, muscle-attachment areas, and intermuscular notch; *C* and *D* radials separated by hexagonal primanal which is widest in lower third and narrowest at summit slightly below level of radial facets or even with them; circlet of distalmost intercalaries composed of eight plates, only *A* radial having one directly beneath it.

Discussion. As noted in the diagnosis above, the radial articular facets are similar to those of many inadunate crinoids. The arms of *P. klapperi,* n. sp. are remarkably similar to those of the inadunate crinoid *Erisocrinus.*

Occurrence. Lower Pennsylvanian (Morrowan)—Upper Pennsylvanian (Missourian), USA (Oklahoma, Missouri, and Kansas).

PLANACROCRINUS KLAPPERI Strimple & Heckel, new species
Text figs. 2-4

Diagnosis. Similar to *Planacrocrinus conicus* Moore & Strimple, 1969, in essential structural features of the calyx other than for the anal series in *CD* interray, which is continuous in *P. conicus.* In *P. klapperi* the two proximal subanals are separated by intercalaries and the distalmost anal plate (primanal) has a broader summit face than found in *P. conicus.*

Ten arms branch with broad axillary primibrachs *1*

FIGURE 3.—Unretouched photographs of holotype (SUI 35580) of *Planacrocrinus klapperi* n. sp. A. Anterior view of crown, B. Posterior view of crown, ×3.5.

FIGURE 4.—Camera lucida drawings of holotype (SUI 35580) of *Planacrocrinus klapperi* n. sp. from Ladore Shale of Linn County, Kansas. A. Anterior (A ray) view of crown, B. Posterior (CD interray) view of crown, ×7.5.

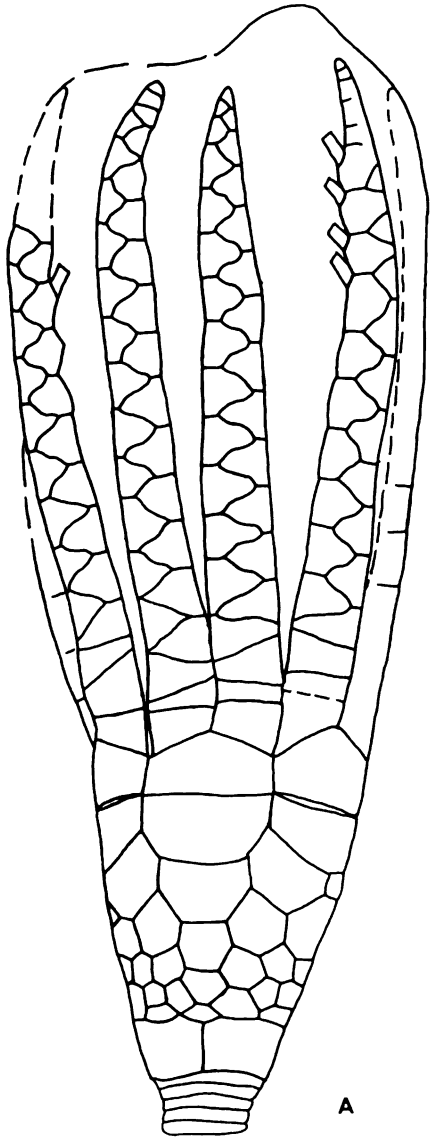

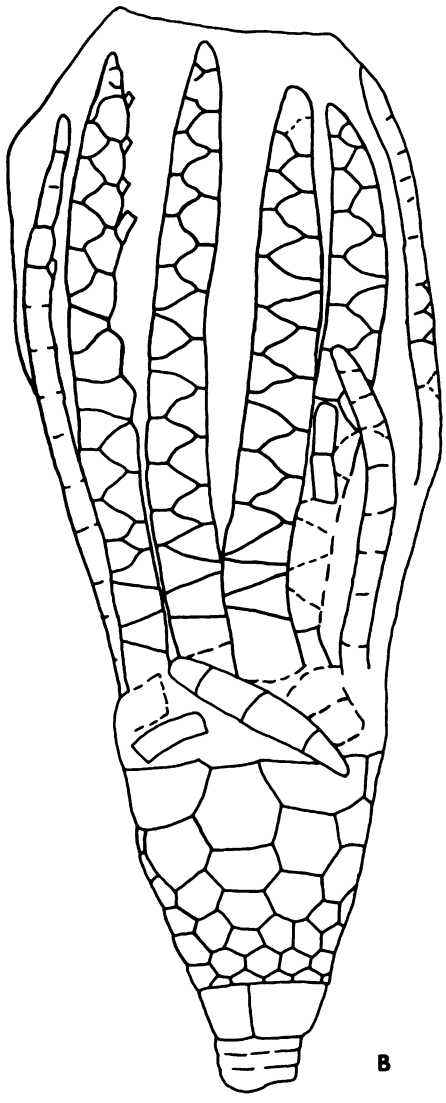

in all rays. Lowermost secundibrachs cuneate but soon become interlocking (equi-biserial). Secundibrachials are pinnular bearing.

Measurements of holotype of *P. klapperi* in millimeters: height of crown 11.2, height of calyx 3.0, width of calyx 2.8, width of stem at calyx 1.0.

Discussion. The steep straight sides of calyx and numerous intercalaries serve to distinguish *P. klapperi* from *P. ambix* and *P. minutus* Moore & Strimple, 1969. In addition to differences previously discussed, *P. klapperi* has proportionately taller basals than found in *P. conicus*. *P. knappi* has an uninterrupted series of anal plates, shorter basals and a broader calyx, all of which distinguish the species from *P. klapperi*.

Types. Holotype SUI 35380, paratypes SUI 42137, deposited in Geology Department Repository, The University of Iowa, Iowa City, Iowa 52242.

Etymology of name. The species name *klapperi* is proposed in honor of Gilbert Klapper, who collected the type specimens from the Ladore Shale in eastern Kansas.

Occurrence. Ladore Shale, Kansas City Group, Missourian Stage, Upper Pennsylvanian Series; north side of Kansas Hwy. 52 in NE¼ SW¼ sec. 23, T. 22 S., R. 23 E., Linn County, Kansas.

REFERENCES

Heckel, P. H. and Baesemann, J. F., 1975, Environmental interpretation of conodont distribution in Upper Pennsylvanian (Missourian) megacyclothems in eastern Kansas: Am. Assoc. Petroleum Geologists Bull., v. 59, p. 486-509.

Meyer, D. L., 1971, Post mortem disarticulation of recent crinoids and ophiuroids under natural conditions: Geol. Soc. America Abst., v. 3, No. 7, p. 45-46.

Moore, R. C. and Strimple, H. L., 1969, Explosive evolutionary differentiation of unique group of Mississippi-Pennsylvanian camerate crinoids (Acrocrinidae): Univ. Kans., Paleontol. Contr. Paper 39, 44 p., 24 figs.

Strimple, H. L., 1975, Middle Pennsylvanian (Atokan) crinoids from Oklahoma and Missouri: Univ. Kans., Paleontol. Contr. Paper 76, 30 p., 17 figs.

RICK DULAS

The Baseline Diagram: A New Water Quality Diagram

INTRODUCTION

Public Law 92-500, the Federal Water Pollution Control Act, particularly Section 102, mandates the Environmental Protection Agency to "prepare or develop comprehensive programs for preventing, reducing, or eliminating the pollution of the navigable waters and groundwaters and improving the sanitary condition of surface and underground waters." These investigations have necessitated the development of a groundwater quality graphic display for use in planning, management, and control processes.

The efficiency of a graphic has long been known; witness the ancient Chinese proverb "A picture is worth a thousand words." There are several components to this efficiency. A good diagram is simple and speedily read; if used more than once it is standardized, and hence comparable. Simplicity is achieved by keeping the information content to a workable level, which for most readers is seven ± two bits of information. This simplicity in turn promotes quick understanding. Standardization of format of a diagram is a must if this diagram is to be used for the comparison and analysis of data. But perhaps the most important feature of a graphic is that it allows an observer to see a pattern which might well have remained obscure if the information were left in some other form. Robinson and Petchenik (1976) say it more succinctly. "Structures are likely to remain hidden until they have been mapped." Anyone who has been confronted by a set of apparently unrelated numbers (Table 1) will appreciate the simplicity and beauty of a well-designed diagram (Fig. 1).

TABLE 1. Selected well records for Scott and Lane counties, in western Kansas. (Data from Hathaway *et al.*, 1975.)

Well Number	Well Location	Date of Collection	SiO_2 ppm	Ca ppm	Mg ppm	Na ppm	K ppm	HCO_3 ppm	SO_4 ppm	Cl ppm	F ppm	NO_4 ppm	Total PO_4 ppm
Scott County													
31	16-31W-31BCB	7/30/74	55	69	25	26	6.0	207	76	42	2.3	26	
32	16-33W-6CCC	8/1/74	35	52	19	29	5.4	196	41	30	2.0	17	.21
35b	16-33W-25BCC	8/1/74	34	44	17	30	5.0	200	37	9.6	2.2	13	
38	16-34W-29CBB	7/31/74	25	43	18	29	4.9	205	47	10.4	1.7	15	
40	17-31W-31BBB	7/31/74	59	80	35	34	7.9	234	114	62	2.1	32	
43	17-32W-31BCB	7/30/74	58	55	24	31	6.2	207	63	34	2.6	23	
48	17-34W-6BCB	7/31/74	26	42	15	30	4.9	209	42	9.9	1.7	13	
53	18-33W-3CCB	7/30/74	60	44	22	30	5.6	208	54	20	2.4	15	
58	18-34W-30DDC	7/31/74	52	56	22	30	6.2	222	53	28	1.8	18	
60d	19-31W-20BAD	8/1/74	29	86	14	28	7.6	262	47	45	.6	22	
62c	19-33W-24ABB	7/31/74	37	125	71	107	10.8	312	483	65	2.1	15	.01
Lane County													
21	16-29W-26CCD	8/1/74	52	53	21	20	5.5	227	39	17	2.3	12	.19
22	16-30W-24DCC	8/1/74	48	52	21	23	5.6	216	43	19	2.3	16	
27	17-29W-36BAA	8/1/74	51	53	24	30	6.8	244	59	19	3.1	12	
29	18-29W-4DAD	8/1/74	56	65	33	28	7.9	245	78	49	4.6	9	.18
30	18-30W-2AAA	8/1/74	57	71	33	41	8.3	242	155	32	3.1	15	

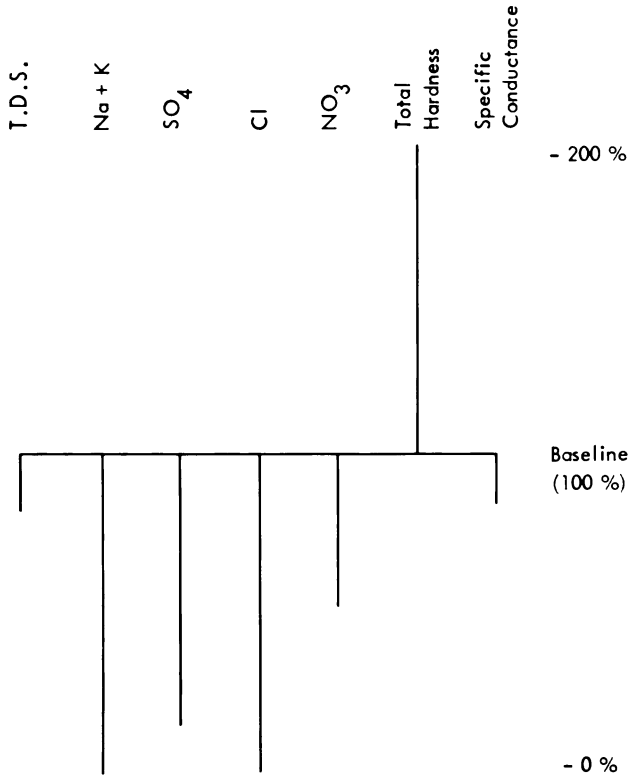

FIGURE 1.—Baseline diagram from Scott Co., Kansas. Well #16 31W 31BCB.

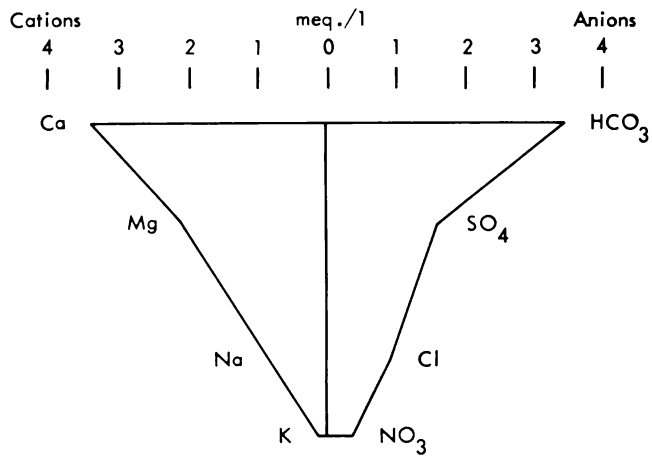

FIGURE 2.—Stiff diagram from Scott Co., Kansas. Well #16 31W 31BCB.

WATER QUALITY DIAGRAMS

Hydrogeology, as a science, has long used diagrams to display groundwater information to assist understanding chemical analyses (Hem, 1959). One of the most frequently used quantitative graphics is the Stiff Pattern (Fig. 2). This display shows cations versus anions radiating from a central spine. The outlying points are then connected by a circumscribing line. The resulting pattern can be compared with other Stiff patterns to ascertain if similarities exist between samples (Stiff, 1951).

Other diagrams in use are Collin's vertical bar graphs, Maucha's radiating vectors, Tickell's radial coordinates, and Piper's tri-linear, examples of which will be found in Fig. 3a-d. These graphics all suffer from several disadvantages. They are difficult to interpret, slow to read, and time consuming to construct. These diagrams are used by chemists and hydrologists in a quantitative way, and as such, have two drawbacks when used to discuss groundwater quality. The first is that these displays have little or no qualitative information for the observer. For instance "Are 80 milliequivalents/liter (meq/l) of calcium good or bad?" If it is good, "Is it twice as good as having 160 meq/l of calcium?" These questions face one when working with conventional chemical analysis diagrams.

TABLE 1. (cont.)

			Fe ppb	Mn ppb	Sr ppm	Ni ppb	Zn ppb	Temperature °C	Total Dis. Solids (180°C)	Hardness as $CaCO_3$ Total ppm	Hardness as $CaCO_3$ Non-Carbonate ppm	Specific Conductance (micromhos at 25°C)	SAR	pH
Scott County														
31	16-31W-31BCB	7/30/74	7	2	1.2	3	4	16.5	425	277	107	695	.68	7.3
32	16-33W-6CCC	8/1/74	8	1	1.0	1	4	16.5	343	211	50	470	.87	7.7
35b	16-33W-25BCC	8/1/74	4	2	.9	2	4	15.5	314	180	16	480	.97	6.8
38	16-34W-29CBB	7/31/74	13	2	.8	4	24	15.5	294	183	15	400	.93	7.2
40	17-31W-31BBB	7/31/74	8	2	1.7	5	4	16.0	438	347	155	830	.79	7.3
43	17-32W-31BCB	7/30/74	11	3	1.1	2	24	16.0	407	238	68	600	.87	6.9
48	17-34W-6BCB	7/31/74	17	2	.8	4	3	17.0	291	167	0	590	1.01	7.6
53	18-33W-3CCB	7/30/74	34	2	1.1	3	12	17.0	352	201	30	762	.92	6.8
58	18-34W-30DDC	7/31/74	26	3	1.2	6	12	16.5	384	234	52	589	.85	6.8
60d	19-31W-20BAD	8/1/74	15	2	.6	3	8	15.0	404	272	57	687	.74	7.0
62c	19-33W-24ABB	7/31/74	32	10	3.5	83	8	17.5	1094	607	351	1510	1.89	7.2
Lane County														
21	16-29W-26CCD	8/1/74	6	2	1.0	0	50	16.0	352	218	32	500	.59	7.6
22	16-30W-24DCC	8/1/74	14	2	1.0	0	23	16.0	356	217	40	520	.68	7.6
27	17-29W-36BAA	8/1/74	17	3	.9	3	21	15.0	392	231	31	601	.86	7.2
29	18-29W-4DAD	8/1/74	8	1	1.1	7	6	18.5	471	300	99	733	.70	7.2
30	18-30W-2AAA	8/1/74	3	2	1.3	11	5	15.5	541	315	117	822	1.00	7.2

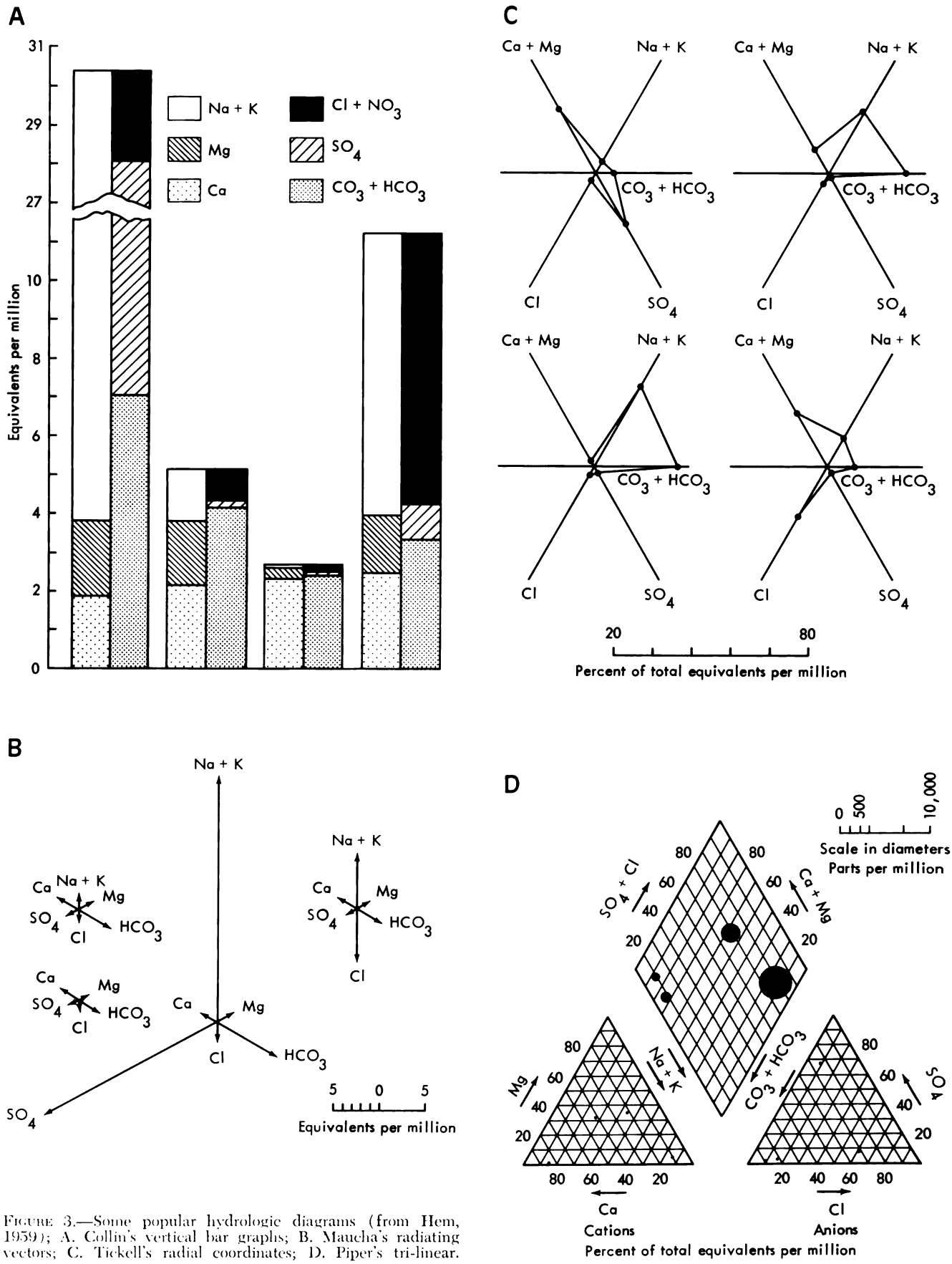

FIGURE 3.—Some popular hydrologic diagrams (from Hem, 1959); A. Collin's vertical bar graphs; B. Maucha's radiating vectors; C. Tickell's radial coordinates; D. Piper's tri-linear.

The second problem is really the other side of the coin. An untrained observer will not only not know "How much is good?", but frequently will not know about the existence of anions or cations. As can be seen, conventional diagrams have some shortcomings.

It would seem then to be an advantage to have a graphic which would not only show quantitative chemical content but also would give a qualitative indication of the water sample. With the development of the Baseline Diagram (Fig. 1), this is now possible. The concept of a non-zero baseline is important as it allows us to depict any deviation from an accepted norm, and tell if something is "good" or "bad" relative to that norm.

The baseline is constructed from the maximum acceptable values of some groundwater quality criteria which are reported in a standard water quality chemical analysis. The value of a non-zero baseline is that it not only allows depiction of the chemical constituents of a water sample, it also allows the observer to make a quality judgment about the water quality relative to the baseline standard. The above and below baseline scaling is predicated on the basis that the baseline represents 100% of the acceptable level of chemical constituents, and that any deviation is some percentage of the baseline value. The scaling is shown in Table 2.

TABLE 2. Scaling factors for the Baseline Diagram.

	T.D.S. mg/l	Na+K "	SO_4 "	Cl "	NO_3 "	Total Hardness "	Specific μmhos/cm. Conductance	
	1500	600	750	750	135	450	2250	300%
	1400	560	700	700	126	420	2100	
	1300	520	650	650	117	390	1950	
	1200	480	600	600	108	360	1800	
	1100	440	550	550	99	330	1650	
	1000	400	500	500	90	300	1500	200%
	900	360	450	450	81	270	1350	
	800	320	400	400	72	240	1200	
	700	280	350	350	63	210	1050	
	600	240	300	300	54	180	900	
Baseline	500	200	250	250	45	150	750	100%
	400	160	200	200	36	120	600	
	300	120	150	150	27	90	450	
	200	80	100	100	18	60	300	
	100	40	50	50	9	30	150	
	0	0	0	0	0	0	0	0%

WATER QUALITY CRITERIA

The seven criteria (Table 3) were chosen because they are readily available from chemical analyses and they communicate water quality information to the untrained as well as the trained observer. Following are the seven constituents and the logic for their selection:

Total Dissolved Solids (T.D.S.)—T.D.S. content is a general indication of water quality, as it reflects the quantity of inorganic salts, dissolved material, and small amounts of organic matter (Sawyer, 1960) left in solution. Generally the higher the T.D.S., the poorer the water quality. According to Sawyer (1960), this measure is associated with unpalatable mineral tastes, possible physiological effects, and high costs due to corrosion.

Sodium Plus Potassium—High sodium can have a deleterious health effect on people who are on a restricted sodium diet, as is the case with some heart patients. Excess sodium, in conjunction with high chlorides, may indicate intrusion of brine into an aquifer or subsurface water body. (In some chemical analyses these two components, sodium and potassium, are reported already summed.)

Chloride—Since chloride will readily combine with different cations to produce several different salts, this chemical is an indicator of the presence of brine and other salts as well as the potential for salinity in groundwater.

Sulphate—This anion occurs naturally in small quantities in surface and groundwater (0 to 100 mg/l), but more often is the result of industrial discharges. Sulphate salts of magnesium and sodium are noted for having a laxative effect on humans if amounts greater than 250 mg/l are found in drinking water.

Nitrate—This has been shown to be the cause of poisoning in young infants (methemoglobinemia) where the nitrogen concentration in drinking water is 10 mg/l or more. High nitrates are also generally associated with high bacteria counts, such as one would

TABLE 3. Baseline criteria, values and authority for selection.

Criteria	*Values*	*Authority*
Total Dissolved Solids	500 mg/l	EPA 440/9-76-023
Sodium plus Potassium	200 "	" " " "
Sulphate	250 "	" " " "
Chloride	250 "	" " " "
Nitrate	45° "	" " " "
Total Hardness	150 "	" " " "
Specific Conductance	750 μmhos/cm	U.S. Salinity Lab.

° Federal law mandates the maximum contaminant level of Nitrate (NO_3) as Nitrogen (N) to be 10 mg/l (EPA 570/9-76-003), but because chemical analyses report Nitrate as NO_3 and not N, a conversion must be made. The factor 4.4268, when multiplied by a quantity of N will yield an equivalent quantity of NO_3 (Lange, 1967). A maximum level of 10mg/l of N will give a baseline level for NO_3 of 44.268 mg/l, which is approximated by 45 mg/l.

find with effluent intrusion into the groundwater from sources such as feedlots, spectic-tank leakage, or sanitary landfills.

Total Hardness—This is a general measure, the greater part of which is usually carbonate hardness. Although not usually a health problem, carbonate waters can be an economic problem as they tend to cause buildup of scale in pipes and valves necessitating expensive repair or replacement.

Specific Conductance—Conductance is a measure of the concentration of soluble salts, and as such is used to gauge the acceptability of irrigation water. "In general, waters with conductivity values below 750 mhos/cm are satisfactory for irrigation, although salt sensitive crops may be adversely affected by conductivity values in the 250 to 750 mhos/cm range" (U.S. Salinity Laboratory, 1951). Conductance is also a readily available field test which enables a worker to

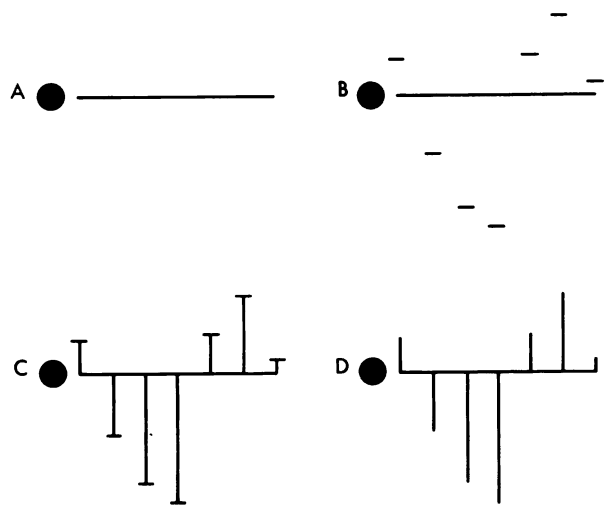

FIGURE 4a-d.—A method of construction used at the Kansas Geological Survey.

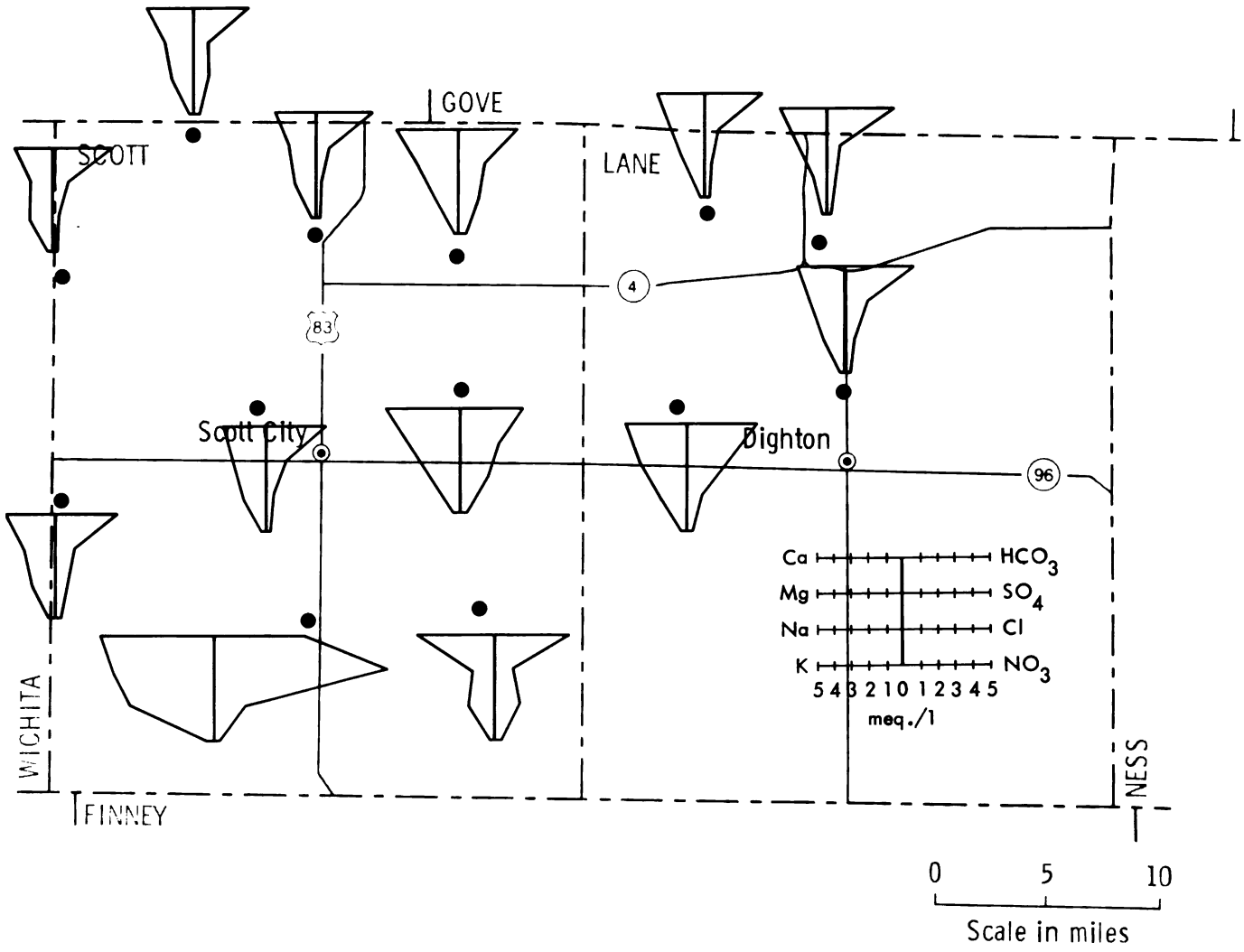

FIGURE 5.—Stiff patterns of selected wells in Scott and Lane counties, Kansas.

compare a new sample with previously analyzed samples quickly and easily.

Although one could choose other criteria, these seem to give an accurate picture of groundwater quality as it relates to the several areas of potential health hazards, industrial pollution, and irrigation hazards.

USE/CONSTRUCTION

The Baseline Diagram is easily drawn using squared or graph paper, 0.1 inch squares being most suitable. Figures 4a-d show a method of construction which has been found useful at the Kansas Geological Survey.

Figure 5 is a portion of a map of western Kansas using Stiff patterns to portray groundwater quality information. Figure 6 is the same area but utilizing instead the Baseline Diagram. As can be seen, the new graphic is better able to convey water-quality information to the reader by the simple observation, "the more bars below and the farther they are below the baseline the better the water."

SUMMARY

This new diagram would seem to have some advantages for use in groundwater analysis and reporting. It is speedily and easily read, yielding quality information to an untrained observer, i.e., the more bars and the higher they are above the line the poorer the water quality. It also allows quick comparison between the samples as there are three visual clues for pattern recognition: left to right sequence of bars, length of bars, and location and length of bars above or below the baseline. In short, this is a new tool for analyzing and displaying groundwater quality information quickly and efficiently.

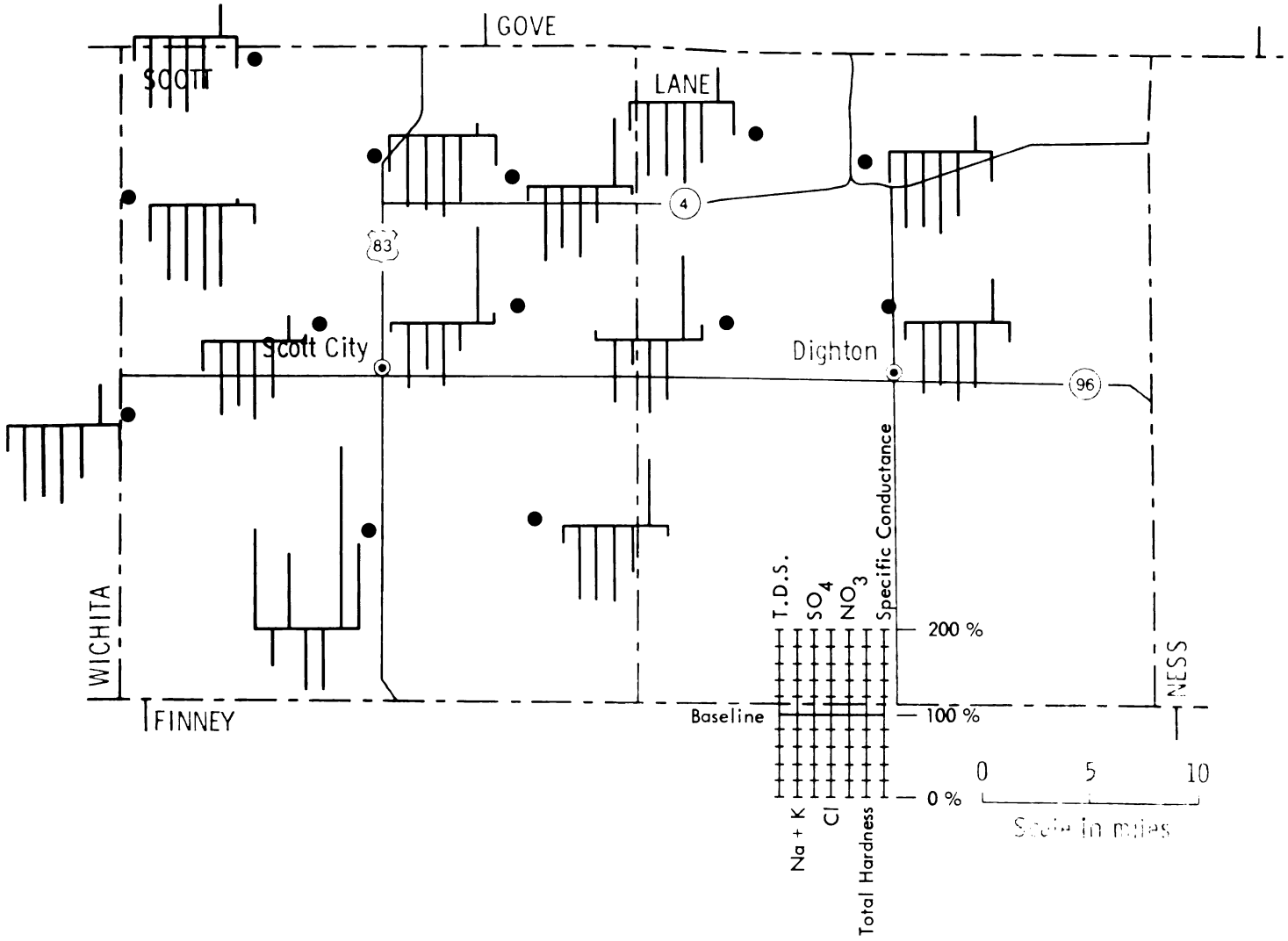

FIGURE 6.—Baseline diagrams of selected wells in Scott and Lane counties, Kansas.

BIBLIOGRAPHY

Environmental Protection Agency, 1976, National Interim Primary Drinking Water Regulations. EPA # 570/9-76-003. G.P.O.: Washington, D.C.

Environmental Protection Agency, 1976a, Quality Criteria for Water. EPA # 440/9-76-023. G.P.O.: Washington, D.C.

Hathaway, L. R., Magnuson, L. M., Carr, B. L., Galle, O. K., and Waugh, T. C., 1975, Chemical Quality of Irrigation Waters in West-Central Kansas. K.G.S. Chemical Quality Series 2. Ks. Geol. Survey, Univ. of Kansas: Lawrence, Ks.

Hem, John D., 1959, Study and Interpretation of the Chemical Characteristics of Natural Water. U.S.G.S. Water Supply Paper 1473. G.P.O.: Washington, D.C.

Hernandez, John W., and Barkley, William A., 1976, The National Safe Water Drinking Act. WRRI Report No. 071. New Mexico Water Resources Research Institute: Las Cruces, N.M.

Lange, J., 1967, Lange's Handbook of Chemistry. Revised 10th ed. McGraw Hill Book Co., Inc.: New York, N.Y.

Robinson, Arthur H., and Petchenik, Barbara Bartz, 1976, The Nature of Maps. Univ. of Chicago Press: Chicago, Ill.

Sawyer, C. H., 1960, Chemistry for Sanitary Engineers. McGraw Hill Book Co., Inc.: New York, N.Y.

Stiff, H. A., 1951, The Interpretation of Chemical Water Analysis by Means of Patterns. Journal of Petroleum Technology, v. 3, no. 10.

U.S. Salinity Laboratory, 1951, Diagnosis and Improvement of Saline and Alkali Soils. U.S.D.A. Handbook No. 60, 160 pp. G.P.O.: Washington, D.C.

U.S. Congress, 1972, Public Law 92-500: Federal Water Pollution Control Act Amendments of 1972. G.P.O.: Washington, D.C.

DAVID A. GRISAFE

Some Physical Properties of Sintered Mixtures in a Bentonite Clay—Volcanic Ash System

ABSTRACT

The optimum firing range (based on firing shrinkage and porosity measurements), thermal expansion, and transverse modulus of rupture were determined for mixtures of volcanic ash (Norton County) and bentonite (Phillips County) which had been pressed and sintered. The clay and clay-ash mixtures used throughout this study mature in the vicinity of 1100° C. The mean linear coefficient of expansion varies from approximately 40×10^{-7} inches/inch/°C for a 80 percent (by weight) ash body to around 61×10^{-7} inches/inch/°C for a 100 percent bentonite body. The transverse modules of rupture vary from very weak strengths of 300 psi for underfired samples to several thousand psi for mature samples. Increasing the bentonite to ash ratio increases both the strength and thermal expansion of the bodies. Bentonite bar specimens sintered at 1100°C possessed a strength of over 6,000 psi.

Small specimens of these materials can be pressed and then heated to 1100°C in one hour without apparent cracking. Such bodies have potential for brick and especially tile.

INTRODUCTION

Considerable amounts of volcanic ash and bentonite clay (formed by the weathering of volcanic ash) are present in Kansas, both materials have limited specialized uses. This study was undertaken to determine whether, after firing, such bodies have suitable properties to be used for brick and/or tile production. The results using volcanic ash from Calvert, Kansas, in Norton County and bentonite from drill hole Adee #2 in adjacent Phillips County are given in this paper.

Procedure

Bentonite (−200 mesh) and volcanic ash to bentonite ratios of 0.25, 0.67, 1.5 and 4.0 were weighed into jars and mixed dry by rolling for one-half hour. One-quarter inch diameter pellets of these mixtures were formed using a steel pellet die and pressing at 10,000 psi on a Carver press. Pellets of each mixture were placed directly under thermocouples in a Glo-Bar heated gradient furnace and were fired using a three and one-half hour rise (at which time the hottest portion of the furnace reached 1200°C) and then soaked or held at temperature for 30 minutes. Afterwards, diameters were measured and the percent shrinkage was calculated and used to determine the approximate maturing range.

In order to measure the transverse strength and expansion after firing, it was necessary first to press bar specimens (1 cm × 10 cm × 0.5 cm thickness) of the above mixtures. Because the high percentage ash mixtures could not be pressed in the dry state, five percent (by weight) water was added to all mixtures as a binding agent. The mixtures were placed in sealed containers for several days to insure a homogeneous moisture content prior to pressing. Bars were formed in a steel bar mold by pressing at 5,000 psi on the Carver press. The bars were fired in a Glo-Bar kiln at desired temperatures and times. After firing, the percent linear shrinkage and apparent porosity (ASTM procedures) were determined. The mean linear thermal expansion coefficient was derived from the fused silica dilatometer technique while the transverse modulus was obtained using the minimum load rate (10 pounds per second) on a Dillon Strength Tester.

Results

Table 1 lists the chemical analyses of the bentonite and volcanic ash used throughout the study. Both of these materials are considered Pliocene in age. A comparison of the oxide contents indicates that portions of alkali and silica were removed during the weathering of ash to bentonite, which in turn enriched

TABLE 1. Chemical Analyses of Bentonite (Phillips County: Sec. 11, T1S, R18W) and Volcanic Ash (Norton County: Sec. 25, T2S, R22W).

	Bentonite Adec #2	Volcanic Ash NNV #1
SiO_2	61.6	72.7
Al_2O_3	15.7	11.2
Fe_2O_3	6.1	2.0
TiO_2	0.6	0.4
CaO	1.0	1.4
MgO	1.3	0.1
K_2O	3.6	5.6
Na_2O	0.3	2.2

TABLE 2. Percent Shrinkage* of Pellets as a Function of Temperature (°C) and Composition.

Approximate Firing Temp.	Ash/Clay Ratio 1/4	2/3	3/2	4/1
1195	−2.8	−4.0	0.4	9.2
1180	−2.8	−4.8	−2.0	10.4
1125	6.4	7.6	10.4	14.4
1040	7.6	8.0	8.8	9.2
925	0.8	1.2	0.8	0.8
830	−1.6	−1.2	−1.2	−0.8

* Negative values indicate expansion relative to initial length. This expansion is often observed in clay-containing bodies fired at low temperatures. Negative values at high temperatures are due to bloating that occurs during overfiring.

the clay in alumina. The major fluxing components in these materials are the alkali and iron oxides. The clay contains four percent less alkali but four percent more iron relative to the ash. Based on the chemical analyses, one might predict some similarity in the physical properties of sintered mixtures in this system.

The percent shrinkage from the gradient firings as a function of the sintering temperature and composition is given in Table 2 while Figure 1 plots these results. The significant feature derived from this data is that the optimum firing (maturing) temperature, marked by the maximum shrinkage, increases only slightly with increasing ash content and all compositions mature in the vicinity of 1100°C. This firing behavior is not unexpected in view of the chemical similarity between the bentonite clay and volcanic ash. The percent firing shrinkage also increases with increasing ash content. As shown in Figure 1, the maturing range of these bodies is relatively narrow; this presents a drawback to the use of these bodies for industrial applications.

X-ray diffraction analysis of bar specimens of these mixtures fired to maturity indicates that little crystalline material remains: the bars are essentially a glassy

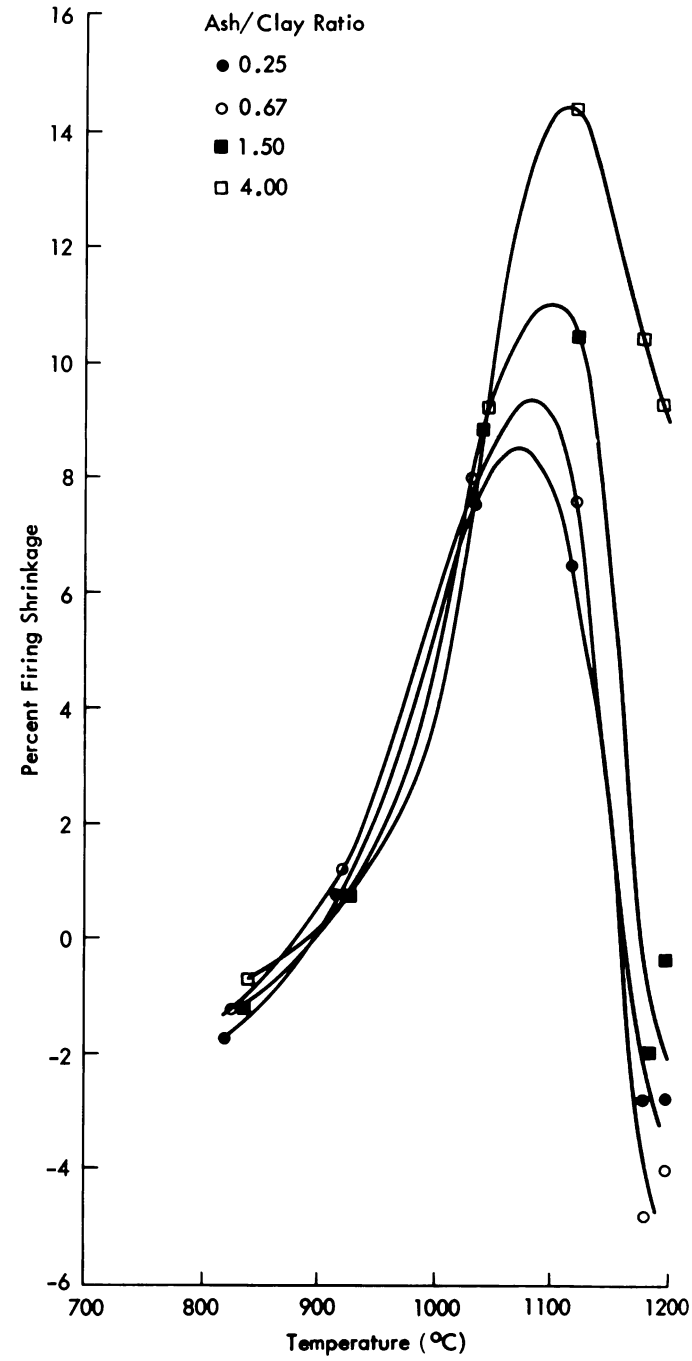

FIGURE 1.—Percent shrinkage as a function of firing temperature for pellets of volcanic ash—bentonite mixtures subjected to gradient firings.

phase containing very small amounts of α-quartz. The amount of crystalline quartz present decreases with increasing ash content due to the glassy nature of the volcanic ash.

Table 3 lists the percent linear firing shrinkage and percent apparent porosity of bar specimens, used for subsequent thermal expansion and transverse strength measurements, as a function of the sintering tempera-

TABLE 3. Percent Linear Firing Shrinkage (LFS) and Percent Apparent Porosity (AP) of Bar Specimens as a Function of Sintering Temperature (°C), Time (Hours), and Composition.

Sintering Temp./Time	Ash/Clay Ratio	1/4		2/3		3/2		4/1		Dry 1/4	
		LFS	AP	LFS	AP	LFS	AP	LFS	AP	LFS	AP
1000/4		7.1	15.8	7.2	19.1	6.8	25.2	6.7	27.0	6.6	27.0
1050/4		10.5	6.2	10.7	7.7	11.0	12.8	11.9	18.0	10.6	13.4
1100/4		12.2	1.7	13.0	1.8	15.0	2.0	18.3	1.8	14.6	0.8
1050/8		10.5	3.1	11.0	6.9	12.5	8.3	.....	.....	.....	.....
1075/4		11.4	1.5	11.7	2.7	13.4	5.2	.....	.....	.....	.....
1075/10		12.3	0.9	13.4	.....	15.1	.....	.....	.....	.....	.....

ture, sintering time, and composition. The percent linear firing shrinkage (LFS) was calculated as:

$$\% \text{ LFS} = \frac{L_D - L_F}{L_D} \times 100$$

where L_D and L_F represent dry and fired lengths respectively. The percent apparent porosity (AP) was calculated as:

$$\% \text{ AP} = \frac{W_{satd} - W_D}{W_{satd} - W_{sus}} \times 100$$

where W_D, W_{satd}, and W_{sus} signify the dry, saturated, and suspended weights respectively. The latter two weights were obtained from bars which had been soaked overnight in water and then boiled four hours in accordance with ASTM testing procedures.

Table 3 shows that as one approaches maturity for a given composition, the sintering temperature and/or sintering time increases the linear shrinkage and decreases the apparent porosity. Note that the mature specimens for a given composition show the maximum shrinkage and relatively zero porosity.

The thermal expansion of these bodies are similar in their general nature. Table 4 lists some typical expansion coefficients of these materials. The coefficient, specifically the aggregate mean linear thermal expansion coefficient, α_m, is expressed in units of inches/inch/°C and is calculated from the expression:

$$\alpha_m = \frac{\Delta L}{L_0 \, \Delta T}$$

where ΔL is the change in length of the bar specimen during heating, L_0 is the initial length of the bar (at room temperature) and ΔT is the change in temperature or temperature range over which the change in length is measured. Table 4 shows that for a given composition, little variation in α_m occurs as a function of the sintering temperature. The coefficient for a given composition is slightly larger when the body is sintered at 1100°C compared to 1000°C because the lower temperature results in more porosity and therefore probably less grain to grain contact.

Increasing the clay-to-ash ratio increases the thermal expansion of these materials. Figures 2 and 3 illustrate typical expansion curves for bar specimens previously sintered at 1000° and 1100°C for four hours respectively. From room temperature to 925°C, the expansion coefficient of mature bodies varies from around 40×10^{-6} for a 20 percent by weight clay body to around 60×10^{-6} for the pure bentonite. The variation in expansion as a function of composition is relatively small for this binary mixture system, again presumably due to the chemical similarity of the two (alkali aluminosilicates).

The inflections on the expansion curves in Figures 2 and 3 in the vicinity of 600°C are due to the $\alpha \leftrightarrow \beta$ quartz transition. These inflections and volume changes are quite small compared to a typical quartz sample such as that shown for a chert specimen in Figure 4. All sintered clay-ash compositions contain a small amount of α-quartz, as measured by x-ray diffraction, and the amount of quartz decreases with in-

TABLE 4. Mean Linear Thermal Expansion Coefficient ($\alpha_m \times 10^{+6}$ in/in/°C)° for Bentonite—Volcanic Mixtures.

Sintering Temp./Time	Ash/Clay Ratio	Pure Bentonite	1/4	2/3	3/2	4/1	Dry 1/4
1000/4		.....	5.39	4.83	4.17	4.06	5.11
1050/4		.....	5.78	5.22	4.44	4.17	5.68
1100/4		6.06	5.78	5.33	4.67	4.39	5.61
1050/8		.....	6.06	5.44	4.67	.....	.....
1075/4		.....	6.11	5.56	4.72	.....	.....
1075/10		.....	5.56	5.17	4.22	.....	.....

° The actual expansion, for example for bentonite, is 6.06×10^{-6} in/in/°C. The α_m values have been multiplied by 10^6 for ease of presenting the data.

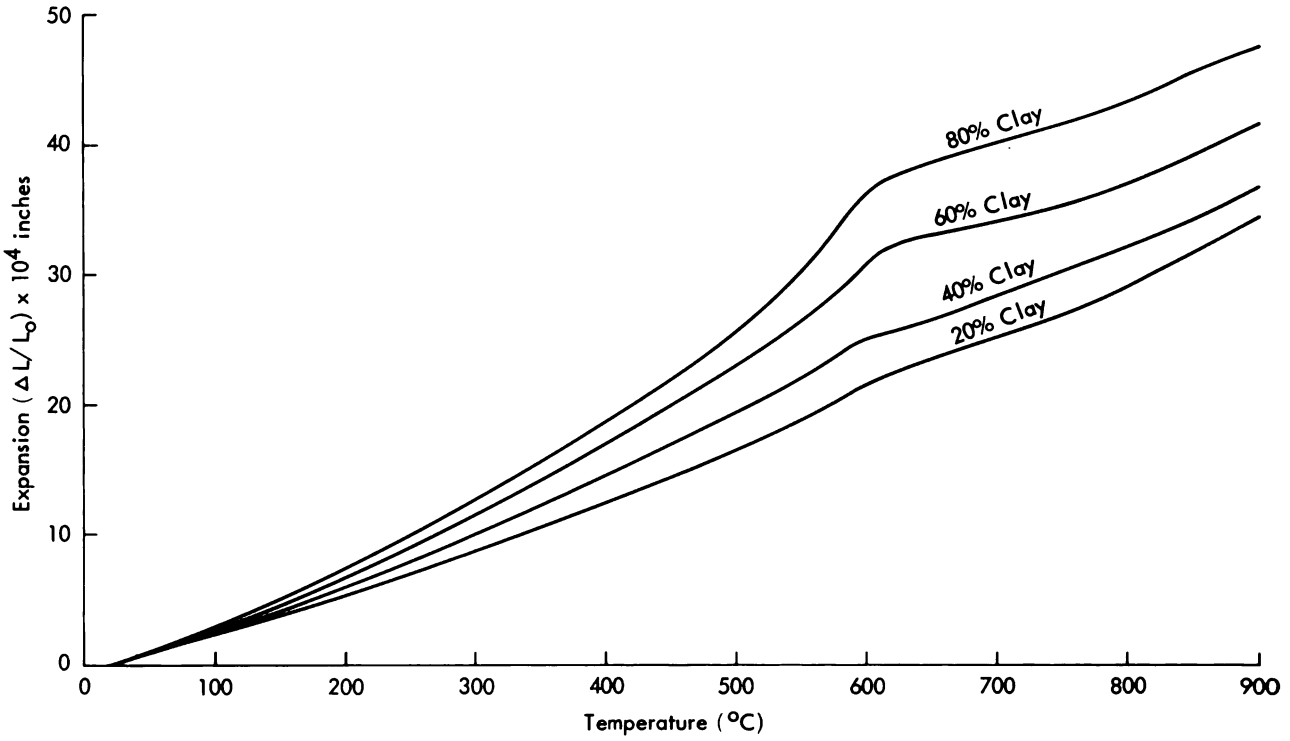

FIGURE 2.—Thermal expansion of bentonite—volcanic ash mixtures after sintering at 1000°C for four hours.

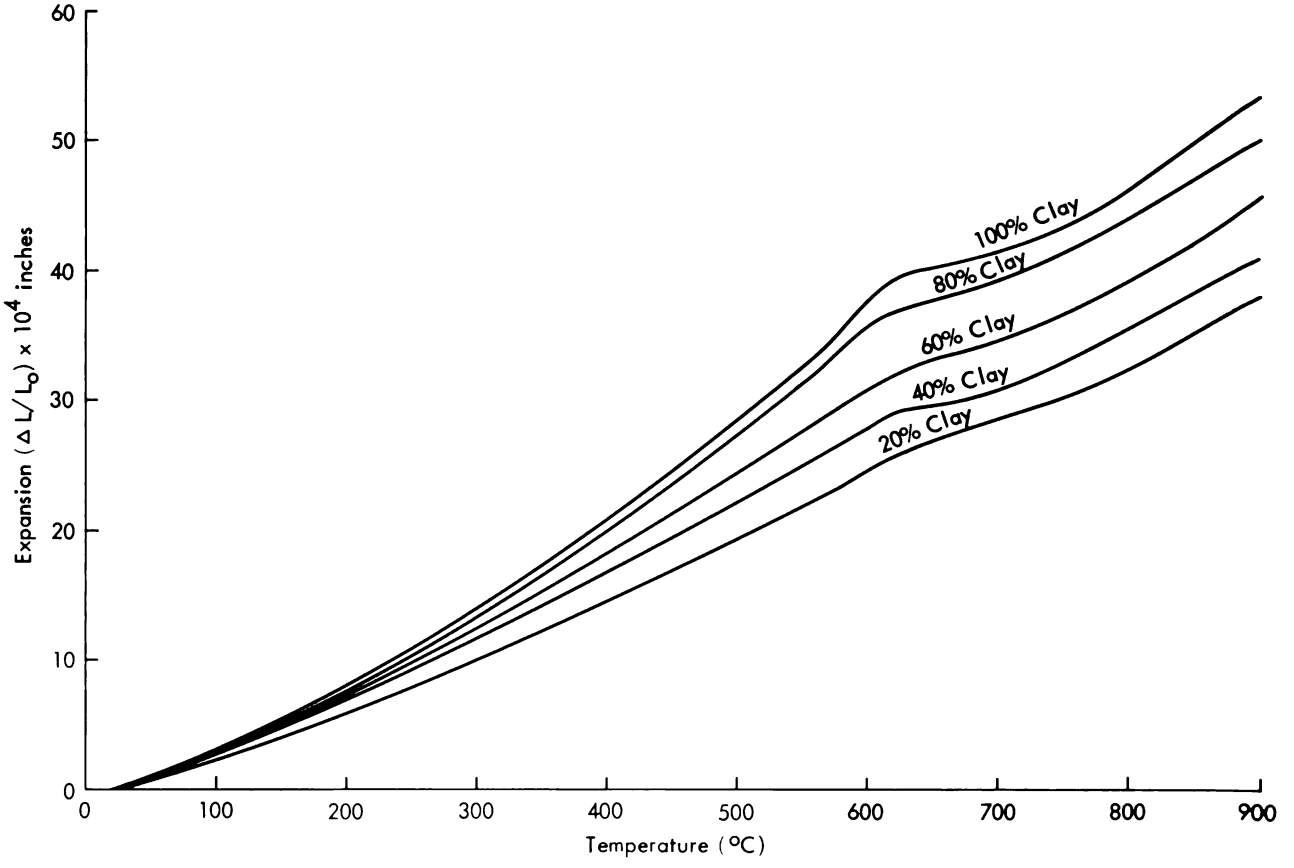

FIGURE 3.—Thermal expansion of bentonite—volcanic ash mixtures after sintering at 1100°C for four hours.

creasing ash content. As a result, at temperatures below 600°C the coefficient of expansion decreases with increasing ash content because (see Figure 4) the expansion of α-quartz is relatively large. The small amount of α-quartz and consequent small volume change resulting from the $\alpha \longleftrightarrow \beta$ quartz inversion would be beneficial in making brick or tile because volume changes produced by crystallographic transitions can cause cracking.

The thermal expansion curves determined at the K.G.S. of another bentonite after sintering show the presence of significant amounts of cristobalite. This form of silica is undesirable in ceramics in large quantities because it undergoes a large volume change at low temperatures and may cause cracking in the ceramic product. By contrast, the bentonite used in this study appears ideal.

The transverse modulus of rupture, M_R, is expressed in units of pounds per square inch (psi) and for bar specimens is calculated from the formula:

$$M_R = \frac{3PL}{2bd^2}$$

where P is the load (exerted perpendicularly to the long axis of the bar) required to break the bar, L is the span of the specimen under stress and b and d are the breadth (width) and depth (thickness) respectively of the bar.

The strength of these bodies is dependent upon the composition, firing temperature, and firing time. Table 5 summarizes the modulus of rupture values for these materials. Each value represents the average of six specimens. The strength increases with an increase of bentonite concentration and an increase in firing temperature between 1000° and 1100°C. Longer soaking times also improve the strength. Up to the maturing temperature the effect of increased temperature and/or soaking time is to produce a denser or less porous body resulting from increased sintering (time and temperature dependent).

Although the sintering mechanism is outside the scope of this work, one can assume that sintering is primarily accomplished by the development of a liquid or glassy phase. The lack of components with high vapor pressures, e.g., alkali halides, suggests that vapor transport plays an insignificant role during the sintering of these materials.

Table 5. Transverse Modulus of Rupture (psi) as a Function of the Sintering Temperature (°C), Time (Hours), and the Composition.

Sintering Temp./Time	Ash to Clay Ratio	Pure Bentonite	1/4	2/3	3/2	4/1	Dry 1/4
1000/4			1520	1130	420	270	320
1050/4			2780	1950	1740	1620	1850
1100/4		6400	4700	3650	3020	1850	4420
1050/8			3780	3550	2310		
1075/4			4720	3480	2550		
1075/10			5350	3180	2930		

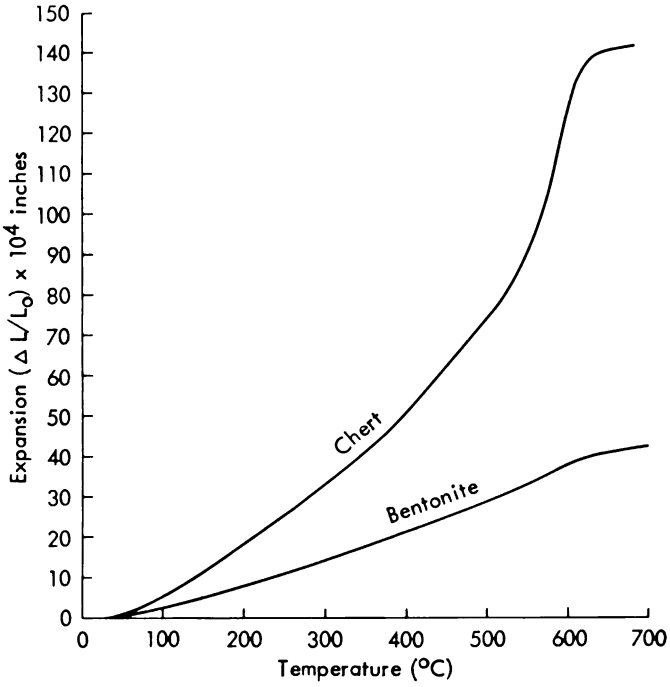

Figure 4.—Comparison of the thermal expansion of bentonite (sintered at 1100 C, four hours) and chert (α-quartz).

The question arises as to why the strength for a given firing temperature and time increases with increasing clay content. Since all compositions fired around 1100°C have negligible apparent porosity, one can say that the increase in strength with increasing bentonite is due to one or more of the following reasons: (1) an increased strength of the glassy matrix, (2) fewer sealed pores or a more favorable sealed pore distribution, and (3) a possible development of small amounts of intertwined mullite needles. It is likely that (1) and/or (2) are the major factors giving rise to the increased strength since mullite was not detected in x-ray diffraction patterns.

The crushing or compressive strengths of well-sintered specimens in this study could not be determined. Attempts to crush were unsuccessful, indicating their strengths were greater than 60,000 psi, the maximum measurable values on the Dillon Strength Testing Instrument.

Several rod specimens of the clay-ash mixtures were extruded. The non-plastic ash prevented the drying cracks which often occur when pure bentonite bodies are extruded.

In general, extrusion produces greenware of a higher density than dry pressing. The water addition necessary for extrusion acts somewhat like a lubricant in that it imparts flexibility to the body and allows particles to slide past one another and form a denser arrangement. Thus, in theory, extrusion should allow one to obtain maturity at a lower firing temperature and/or a shorter soak period.

The bodies in this system behaved in the predicted manner: extruded clay-ash mixtures matured around 1070°C with a three-hour soak, whereas extruded specimens fired at 1100°C (maturing range for dry pressed specimens) were slightly bloated and, hence, overfired. The bloated samples had a slightly lower transverse strength than samples fired at 1070°C.

Perhaps the most significant feature of this test was the strength values obtained from extruded rods and dry-pressed bars. The modulus of rupture for a cylindrical rod is calculated from the formula:

$$M_R = \frac{8PL}{\pi D^3}$$

where P is the load required to break the rod, L is the span under stress and D is the rod diameter. For a three-inch span the formula becomes

$$M_R = 7.64P/D^3$$

The modulus of rupture obtained from rods of the 60/40 clay to ash ratio bodies when fired at 1065°C/3 hours approached 5,000 psi. This value represents a striking improvement over the 3650 psi value obtained from dry-pressed bars of the 60/40 mixture fired at 1100°C (see Table 5).

SUMMARY

An examination of the firing properties, thermal expansion and strength has been completed for a bentonite clay (Phillips County, Adee #2)—volcanic ash (Calvert, Ks. in Norton County) binary system. The system served as an excellent example of classical ceramic behavior.

For all dry-pressed compositions, as one obtains maturity, one observes a maximum firing shrinkage and zero apparent porosity. From 1000°C to the optimum firing temperature, 1100°C, one observes increases in strength and thermal expansion for a given composition. In a given thermal treatment, an increase in ash content reduces both the strength and thermal expansion. Pure bentonite gives a strength value of over 6,000 psi and a mean linear thermal expansion coefficient of 6×10^{-6} in/in/°C. By contrast, an 80 percent (by weight) ash content at maturity gives a strength value of only 1850 psi and an expansion coefficient of 4.4×10^{-6} in/in/°C.

All bodies in this system have relatively narrow firing ranges that would require close control of kiln temperatures. However, these bodies can be subjected to rapid firing in an electric shuttle kiln lined with refractory fiber which represents a substantial savings in time and production costs. The adequate strength, moderate expansion, and rapid firing give this system potential for brick and especially floor tile production because the latter can be rapidly pressed with little or no binder and being thin, can be fired quite rapidly.

In conclusion, bodies in this system appear to have potential for use in a tile production facility, possibly in northwestern Kansas where substantial reserves of ash and bentonite are located.

MAYNARD P. BAULEKE

How to Solve the Problems of Body Cracking and Glaze Popping in Stoneware Bodies

THE PROBLEMS

Stoneware potters often complain about two problems occurring with their ware; it is cracked when removed from the kiln or the glaze pops off the surface after the glaze is fired. A body used for years may suddenly develop these problems. The potter assumes that nothing has changed in the method of handling or firing the body. This is probably true, but some small change in final fired-body composition has occurred. This problem is not new; it has been going on as long as potters have been firing stoneware. It's just that often one forgets how the old problems were solved. Most pottery books mention the cracking problem and imply that if you are careful and don't anger the "pottery gods" too often, the problem can be lived with.

It is the purpose of this note to give some insight into the source of the trouble and some steps that may be taken to correct it. No specific body compositions are referred to, nor is a typical composition listed, because there are so many variations of stoneware compositions in use. Only ideas for problem solutions are presented. How the ideas presented are used to solve your problem will depend upon how much control you have over the stoneware body formulation. Sometimes the simplest solution is to change to another clay body.

CAUSE OF THE PROBLEM

X-ray diffraction analysis and thermal expansion measurements of the broken ware always show an excessive amount of the high temperature phase of quartz known as cristobalite to be present. Vitrified stoneware expands in size when heated and shrinks when cooled. This change in length is called thermal expansion.

The troublesome thermal expansion curve for the cristobalite form of quartz is shown in Figure 1 along with the thermal expansion of other phases normally present in vitrified stoneware. Note the very large percent linear change for cristobalite at about 200°C (392°F). This is the cause of the trouble as it changes from the β to α form during cooling. The α and β refer to different arrangements of the atoms within the crystal structure, β always referring to the high-temperature structure in American literature. (It is common in European literature to reverse the meaning of the symbols.) This reaction happens upon heating and cooling each time the ware is thermally cycled. If the ware comes out of the kiln broken, the trouble is caused by the β form changing to the α form causing it to break in the first cooling period. The quartz expansion curve shows a similar behavior, but the transformation occurs at a higher temperature and is of a lesser magnitude than that of the cristobalite so it is less troublesome in most bodies. The glass expansion is characteristic of a glass in that the expansion is linear up to a region just below its softening temperature. Mullite has the ideal thermal expansion curve for a stoneware body that is to be used as ovenware. Note the lack of any irregularities in the curve. It is smooth and continually increasing with increasing temperature.

SOURCES OF CRISTOBALITE

Cristobalite is the high-temperature form of quartz with its region of equilibrium stability above 1470°C (2678°F). How can this cause trouble if the body has never been fired higher than cone 9 or 10, a maximum of 1285°C (2345°F)? The 1470°C temperature applies only if you are starting with pure quartz and converting it to cristobalite. A stoneware body is not

pure quartz but is mostly made up of clays which contain some free quartz. Note that in the expansion curves for stoneware bodies in Figure 2 the α and β transformation for quartz is still visible, showing that much of the original quartz was not transformed to cristobalite or dissolved in the glass phase.

Most of the stoneware bodies are formulated around clays containing the clay mineral kaolinite, which when heated undergoes the following set of reactions:

$Al_2O_3 \cdot 2SiO_2 \cdot 2H_2O$ Kaolinite	450-600°C →	$Al_2O_3 \cdot 2SiO_2$ Amorphous Kaolinite	$+ 2H_2O$
$2[Al_2O_3 \cdot 2SiO_2]$	900-1000°C →	$2Al_2O_3 \cdot 3SiO_2$ Spinel structure° phase	$+ SiO_2$ Amorphous
$3[2Al_2O_3 \cdot 3SiO_2]$	1050-1200°C →	$2(3Al_2O_3 \cdot 2SiO_2)$ Mullite	$+ 5SiO_2$
SiO_2 Amorphous	1100-1200°C →	SiO_2 β-cristobalite	

It is the last reaction that causes the problem. If it can be prevented, or retarded, the amount of cristobalite will be held to a minimum. Why the cristobalite forms at temperatures below its temperature of stability is one of the interesting quirks of the crystallization phenomena. Amorphous silica has a random arrangement of silicon and oxygen ions similar to that of silica glass. However, this is a highly unstable state for the 1285°C temperature and the ions will arrange in the most loosely packed crystalline arrangement possible, which is β-cristobalite. Once in this form, the change to another crystalline arrangement is normally slow. Thus, there is a good chance of having some cristobalite present in the fired ware.

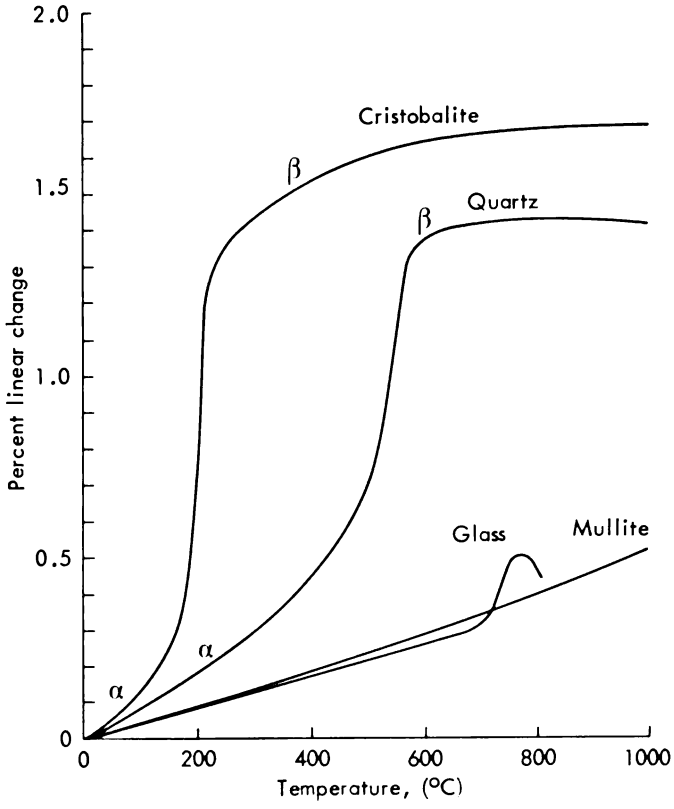

FIGURE 1.—Thermal expansion curves for the phases present in fired stoneware.

At the same time the transformation of the amorphous silica into cristobalite is occurring, another reaction is going on that is removing some of the amorphous quartz which is reacting with the melting fluxes to form the liquid phase that is vitrifying the body. Since the atomic arrangement of amorphous silica is closer to that of the liquid phase than is that of the crystalline quartz, the amorphous silica will be dissolved at a faster rate than the other crystalline forms of quartz. The liquid phase can only dissolve a certain amount of silica, depending upon its overall chemistry. The remaining silica is available for crystalline phase formation. If the liquid phase becomes supersaturated with silica as it cools, there is a high probability that the excess will precipitate out as crystalline cristobalite. A small amount of cristobalite is beneficial towards developing the proper compressive stress in the glaze to prevent crazing and increase the strength of the fired ware; only an excess causes trouble.

TENSION STRESSES IN THE BODY CAUSE CRACKING

Before suggesting remedies for the problem, let's look at how the thermal expansion behavior of the body can cause both the body cracking and the glaze popping problem. Thermal expansion is the change of the length or volume of the solid as the temperature

° This refers to a spinel crystal structure. It does not mean the compound $MgO \cdot Al_2O_3$, spinel, is formed.

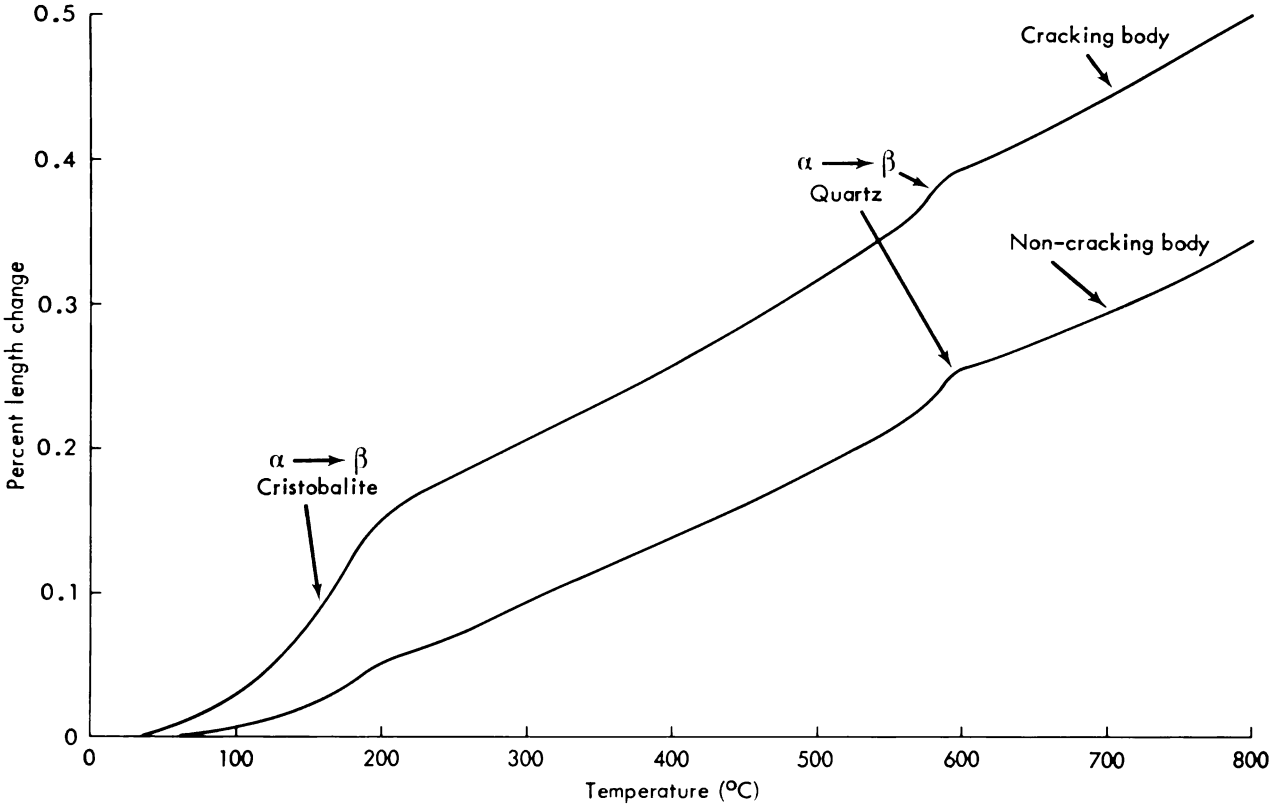

FIGURE 2.—Thermal expansion curves for a cracking and non-cracking fired stoneware body.

changes. Normally a solid expands when heated and shrinks when cooled. A small thermal expansion change means good thermal shock resistance while a large thermal expansion change means poor thermal shock resistance of the body. Why?

A thermal gradient is established in the ware when it is cooled. The slower the cooling rate the smaller is this gradient between the hotter inside and the cooler outside of the wall. The cooler outside wall has contracted more than the hotter interior, creating a tension or pulling apart in the outer wall because the interior is trying to keep it from contracting. Tension forces are building in the outer surface and when this force exceeds the tensile strength of the body, which is quite low, a crack begins and the wall breaks. The problem is dealt with by reducing the rate of cooling or by reducing the thermal expansion value so that it is difficult to establish a large differential of length change during cooling. What makes the α to β transformation so troublesome is that no ions have to move and rearrange to produce the change in volume. The change occurs almost instantaneously by changing a bond angle between the silicon and oxygen ion when the transformation temperature is reached. It occurs over a small temperature range in the expansion curve because it takes time for the interior of the ware wall to reach the transformation temperature. The transformations occur upon both heating and cooling as long as the crystalline phase is present. If you want cristobalite present in fairly large amounts, the cooling rate must be quite slow between 250°C (482°F) and room temperature to prevent the buildup of excessive tensile forces. Close the kiln door during this range, or at least don't let cooling air blow directly onto the ware. How fast the stoneware body can be cooled depends largely upon the thermal expansion behavior below 250°C (Figure 2 shows a fairly linear rate of expansion above this temperature). This does not mean that the body can be cooled from maturing temperature to 250°C in one hour. Find out the limitations of your ware and also the thermal shock limitations of the refractories in your kiln.

According to Lawrence (page 126) cracks originating because of the quartz inversion can be distinguished from cracks caused by the cristobalite inversion. Both cracks will be sharp, but because the cristobalite crack occurred at a much lower temperature, its surface will be dull while the surface of the higher temperature crack will be smooth and glossy.

Porous bodies may have a considerable amount of cristobalite present and still have reasonably good thermal shock resistance because the pore structure retards the spread of the crack. The cracks are still there, but they don't grow and cause immediate fail-

ure. After many thermal cycles, pieces of the ware will develop cracks of major size. Vitreous ovenware should have a minimum of cristobalite material present as the ware has no porous structure to block crack development and growth.

COMPRESSIVE STRESSES IN THE GLAZE CAUSE POPPING

Glaze popping (dunting) also occurs below 255°C because the body is shrinking much faster than the glaze is shrinking. This difference in the two rates of length change causes a large amount of compressive stress to develop in the thin layer of glaze. The glaze buckles and pops off the surface. The cure is to lower the thermal expansion of the body in the last few hundred degrees of cooling temperature. Raising the thermal expansion of the glaze is another solution but it may create crazing problems that the method of lowering body expansion avoids. A good glaze fit occurs when the thermal expansion of the glaze is just slightly less than the thermal expansion of the body in all temperature regions where the glaze is solidly attached to the body. If given a choice, most potters would rather have the glaze craze than pop off the surface.

HOW TO CONTROL THE AMOUNT OF CRISTOBALITE FORMED

Now that we know that cristobalite is causing the problem, here are some steps than can be taken to minimize or control the amount formed.

Reduce Firing Temperature

The maximum amount of cristobalite formed from the decomposition of the kaolinite appears to be in the temperature range of 1250-1300° C (cone 7-10). Lowering the firing temperature without changing the flux content of the body may increase the porosity and may not properly mature the currently used glaze.

Change the Grog Material

Most stoneware bodies contain brick grog which often has well-developed particles of cristobalite present. Such particles are difficult to dissolve in the liquid phase and will act as growth sites for the transformation of the amorphous quartz into cristobalite and for the precipitation of excess silica in the glass phase as cristobalite during cooling. It is best to use grogs low in cristobalite content, such as calcined kyanite or synthetic mullite ($3Al_2O_3 \cdot 2SiO_2$). Some commercial suppliers are using such grogs in their stoneware. Brick grog is often made by crushing scrap bricks; hence, the quality may vary widely from source to source.

Increase or Change the Flux Content

Another method of reducing the cristobalite content is to dissolve the amorphous silica material in the high temperature liquid phase. If the body has five percent potash feldspar present, increase it to ten percent. This will increase the glass content and probably allow a lowering of the firing temperature. It may remove some of the iron color. If iron color is important, try adding three to five percent calcium fluoride (minus 200 mesh) in addition to the flux already present. This flux tends to retain the iron spots and there is a small amount of iron in natural calcium fluoride.

When the flux content is increased, the amount of liquid phase also increases at the maturing temperature, which may cause slumping. Always test fire small quantities of the body before preparing large amounts.

Beware of using fluxes high in sodium oxide content. Sodium oxide may accelerate the rate of conversion of amorphous quartz into cristobalite. Some claim that there is no difference between the use of soda spar and potash spar in stoneware bodies. It is best to use only the potash spar.

Lower the Iron Oxide Content

Why does reduction firing cause more cristobalite to be formed in some bodies than others? The amount of iron oxide (Fe_2O_3) is often the reason. Ferric oxide (Fe_2O_3) is reduced to ferrous oxide (FeO) in the reduction firing. The ferrous oxide melts and penetrates into the amorphous silica structure and promotes the formation of cristobalite. Such a compound is called a mineralizer. Thermal expansion measurements of all iron-containing stoneware bodies showed that reduction firing increased the amount of cristobalite present.

Keep the iron content as low as possible if you fully reduce the ware. If iron spots are important in the glaze, try to formulate the glaze so that the spot material is in the glaze and not derived from the contact of the glaze and the body.

Control Degree of Reduction

Fire under mild oxidation atmosphere and reduce only as necessary to produce the glaze effect needed. It is not necessary to have the body saturated with black carbon into the center of the wall. This does nothing beneficial for the body. A reduction firing should not belch black smoke, as only the carbon monoxide present is affecting the reduction process.

Hold Peak Temperature Soaking Time to a Minimum

The longer the body is held at peak temperature

the more time is available for rearrangement of the silicon and oxygen atoms into the cristobalite structure. This is somewhat balanced by the glass-forming reaction which dissolves more quartz over a longer time period. However, the latter may saturate the glass composition and cause cristobalite to precipitate during cooling. Experiment and find out the best soaking time for the body.

How Much Cristobalite is Allowable?

This is a difficult question to answer as the average potter has no way to measure the quantity present. The best suggestion is to give the fired stoneware a mild thermal shock by removing it from the kiln at 250°C (500°F) and allowing it to rapidly cool to room temperature in a static air condition (no wind blowing across the piece). If it doesn't break, the amount of cristobalite present is not excessive. Figure 2 shows the thermal expansion for two stoneware bodies. The cracking stoneware body shows a rapid increase in thermal expansion between 100 and 200°C. It is this rapid expansion that is cracking the body. The non-cracking body is a similar composition that has been modified by replacing the brick grog with calcined kyanite grog and increasing the potash spar from 5 to 10 parts by weight. Its thermal expansion curve increases at a much slower rate. Both curves shows a small inversion just below 600°C due to the α-β quartz transformation showing that some of the quartz has not been dissolved in the liquid phase nor has it been transformed to cristobalite.

A stoneware body that can tolerate moderate thermal shock will have an expansion curve similar to the non-cracking curve. For non-ovenware items the amount of cristobalite can be increased. Remember that small amounts of cristobalite are not bad as they provide some compression in the glaze and reduce the tendency for glazes to craze.

For a good summary of applied science and the potter I suggest reading CERAMIC SCIENCE FOR THE POTTER by W. G. Lawrence, published in 1972 by the Chilton Book Company, Philadelphia, Pa.